

TMS-EEG based Source Localized Connectivity Signature Extraction by using Unsupervised Machine Learning

Deepa Gupta^{1*}, Member, IEEE, Xiaoming Du², Elliot Hong^{2,3}, Fow-Sen Choa¹, Member, IEEE

Abstract— Transcranial magnetic stimulation (TMS) is gaining increasing attention for therapeutic treatment of mental illnesses. However, a clear understanding of its impact to the underlying brain mechanisms is critical for its effective application. For this, we analyze electroencephalography (EEG) response to TMS subthreshold pulse at the left motor cortex from 6 healthy controls and 6 schizophrenia patients. We use principal component analysis (PCA) along sparse nonnegative matrix factorization (NMF), an unsupervised machine learning technique, on brain connectivity data established by sliding window coherence of EEG based source localized data. The source localization was achieved by using the sLORETA algorithm on our EEG data after artifact removal. This, hence, provides high temporal and spatial resolution in the connectivity analysis results, giving advantage over other neuroimaging modalities. PCA aids in establishing the number of common underlying connected subnetworks (say k) across subjects whereas NMF is employed to derive these k spatial and temporal signature subnetwork response to the stimulus. Within these signatures, we studied motor cortical connectivity and found that schizophrenia patients exhibited sensory gating deficits as compared to controls. These findings can act as potential biomarkers to monitor TMS for clinical therapeutic techniques in the future.

I. INTRODUCTION

Sensory gating deficits are very common in mental illnesses, especially schizophrenia, where the individual lacks the physiological process of filtering out unnecessary sensory information [1], [2]. Therapeutic techniques developed for treating such ailments are still undetermined. Transcranial Magnetic Stimulation (TMS) has recently gained a lot of popularity for the same, however, its consequent effect to the cortical activity is still not clearly understood, which hinders its usage as an effective treatment and raises concerns for safety [3]. Efforts in this direction are better explored with electroencephalography (EEG) given that derivation of causal relationship is impossible without high temporal resolution, which is essential for the

This research was supported by NSF grant ECCS-1631820, NIH grants MH112180, MH108148, MH103222, and a Brain and Behavior Research Foundation grant. *Corresponding author: Deepa Gupta deepag1@umbc.edu

¹Computer Science and Electrical Engineering, University of Maryland Baltimore County, 1000 Hilltop Circle, Baltimore MD 21250.

²Maryland Psychiatric Research Center, University of Maryland Baltimore, 620 W. Lexington St., Baltimore, MD 21201

³Department of Psychiatry, University of Maryland School of Medicine, Baltimore, 655 W. Baltimore Street, Baltimore MD 21201.

given problem statement. EEG is a non-invasive neuroimaging technique that offers high temporal resolution unlike any other neuroimaging technique [4]. Applying this technique with source localization algorithm, a 3D inverse technique to predict source dipoles inside the brain for the given EEG data, improves spatial resolution information for better analysis.

Here, we studied EEG based source localized data in response to TMS subthreshold stimulus administered at the left motor cortex of 6 healthy controls and 6 schizophrenia patients by using machine learning techniques to generate common spatial and temporal signature across controls and patients, which show sensory gating deficits in patients. We discuss our algorithm in the methods section and report our signature findings in the results and discussions section.

II. METHODS

A. Experimental Procedure and data preprocessing

TMS was administered at the left motor cortex of 6 healthy controls and 6 schizophrenia patients. Their EEG response was recorded from 11 cortical electrode sites as shown in Fig. 1 for 60 trials each 4sec apart. EEG was then processed for artifact removal by applying a 1-50Hz band pass filter and a peak to peak threshold value of 100 μ V in a sliding window technique with a window size of 200ms with 50ms shift in MATLAB based EEGLAB and ERPLAB toolbox[5], [6]. The epoch size for each trial was chosen to be 1000ms post 50ms of the TMS pulse to avoid the very noisy part of the data. The epochs with artifacts were discarded.

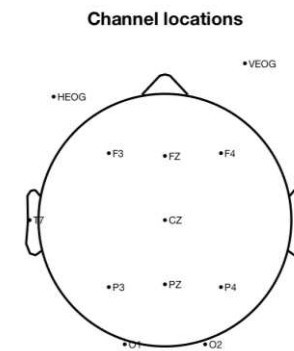


Figure 1 Layout of (approximate) location of electrode sites used for recording EEG response from 12 subjects to TMS administered at the left motor cortex.

B. EEG source localization and connectivity estimation

Source localization was performed on each EEG epoch data by using the sLORETA algorithm[7]. sLORETA, abbreviated for standardized low-resolution brain electromagnetic tomography, is a standard technique to solve the inverse problem at a spatial resolution of 5mm based on the digitized Talairach atlas provided by the Brain Imaging Centre Montreal Neurological Institute[8] to estimate source current density inside the brain for the given EEG data. For each epoch's estimated source current density, a sliding window coherence was calculated. Coherence computation was based on the unambiguous brain interaction approach formulated by Nolte et al[9], which is given as:

$$C_{ij}(f) = \frac{S_{ij}(f)}{\left(S_{ii}(f) S_{jj}(f) \right)^{\frac{1}{2}}} \quad (1)$$

All of these algorithms were implemented by using the open source MNE-Python library[10], [11]. We extended this by implementing a sliding window coherence technique for enabling the analysis of causal temporal dynamics from the 68 estimated sources with a window size of 200ms and 20ms shift over the 1000ms long epoch, resulting in coherence values based on (1) for 2,278 pairs of estimated sources for 41 windows for each subject.

C. Subnetwork Extraction

The 2,278 coherence values over 41 windows for each of the 6 controls were stacked together yielding $A \in \mathbb{R}^{P \times T}$ where P is the number of pairs, i.e. 2,278 pairs from 68 estimated sources ($n(n-1)/2$ where $n=68$ sources) and T are the total number of time windows, which is equal to 246 given that there are 6 controls each with 41 time windows. Given that coherence values range between 0 (least coherent pair) and 1 (most coherent pair), A is a nonnegative matrix that is factorized into two matrices W and H by employing sparse non-negative matrix factorization algorithm, an unsupervised machine learning technique formulated by Kim and Park et al [12], which is given as:

$$\begin{aligned} \min_{W,H} \frac{1}{2} & \left\{ \|A - WH\|_F^2 + \eta \|W\|_F^2 + \beta \sum_{i=1}^T \|H(:,i)\|_1^2 \right\} \\ \text{s.t. } & W, H \geq 0 \end{aligned} \quad (2)$$

where $W \in \mathbb{R}^{P \times k}$ is a subnetwork connectivity matrix i.e. the spatial signature and $H \in \mathbb{R}^{k \times T}$ is temporal expression coefficients i.e. the temporal signature across the subjects (please see the Appendix for our methods' illustration). The common dimension, k is the number of signatures obtained from this factorization. η is a regularization parameter for constraining the connectivity values in W and β is a penalty parameter that is used for enforcing sparsity on the temporal expression coefficients. Based on the dynamic machine learning approach [13], [14], to select a suitable value of k we used PCA as its resulting Eigen-decomposition along the corresponding variance estimation gives an indication of how many underlying patterns or components contribute substantially towards the connectivity dataset A . We take η to be the square of maximal element in A following prior work [12], [14]. We optimize for β by computing the frobenius norm of the error $A - WH$ for varied values of β for the

selected k and selecting the one that yields the minimum error.

Unlike PCA that generates orthogonal components, NMF generates factors that can capture subnetworks that may share some overlaps. Given that brain connectivity overlaps over multiple underlying brain subnetworks, NMF becomes more suitable for our analysis. Chai et al have used similar approach with fMRI studies for analyzing subnetworks in young and adult subjects[14]. However, fMRI is temporally limited and hence, exploring this with EEG based source localized data gives an advantage in investigating brain response to TMS at a high spatial and temporal resolution.

D. Signature analysis metrics

For analyzing the temporal signature H , we averaged time expression coefficients for 41 windows across subjects to understand the transient signature for each subnetwork.

For analyzing the spatial signature W , we reshaped each vector into a 68x68 coherent graph for plotting and better analysis. Then, out of the estimated 68 source dipoles, 6 major regions were shortlisted that majorly belonged to the motor cortex, namely the precentral gyrus, paracentral lobule and the postcentral gyrus in both left and right hemisphere. Coherence of these elements with each other, in each subnetwork (i.e. a vector in W) that was obtained after NMF of A , was averaged to get a measure of within motor cortex ($M1$) connectivity. For example, for a deduced subnetwork $W(r)$, the within motor cortex connectivity will be given by:

$$Conn_{\text{within } M1} = \sum_{i \in |M1|, j \in |M1|} \frac{W(r)_{ij}}{|M1|} \quad (3)$$

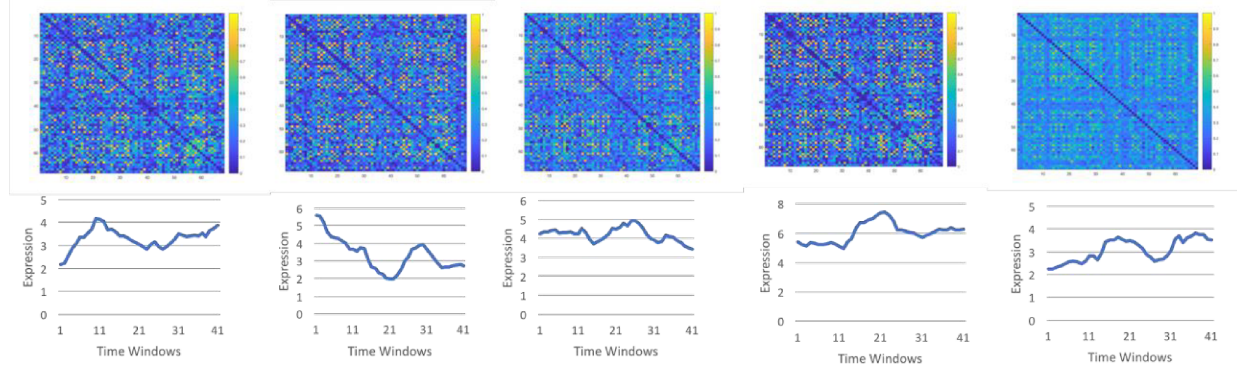
where $|M1| = 6$ i.e. number of nodes or regions belonging to the motor cortex as listed above, r varies from 1 to k (k = total number of factors from NMF as explained in the previous section) and $W(r)$ represents the r^{th} vector i.e. a subnetwork in W . Similarly, connectivity between the motor cortex and the rest of the regions for a given subnetwork, $W(k)$, will be given by:

$$Conn_{\text{with } M1 \text{ and } N} = \sum_{i \in |M1|, j \in |N|} \frac{W(r)_{ij}}{|N|} \quad (4)$$

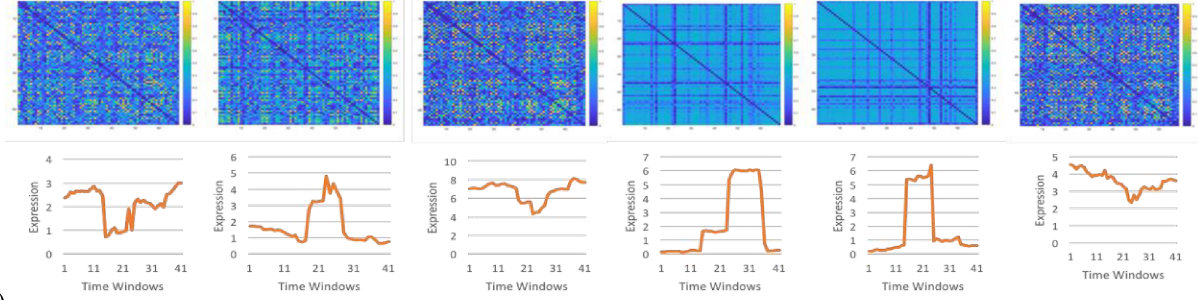
where N represents rest of the brain regions $|N| = 68$ i.e. the number of brain regions or nodes.

III. RESULTS

Following our methodology, we obtained a total of 6 spatial and temporal signatures for patients whereas for controls we got 5 spatial and temporal signatures as shown in fig. 2. The number of controls and patients are same, which means the dataset was the same size to begin with despite which our machine learning approach yielded more factors for patients than controls. Moreover, the temporal expression coefficients are overall unstable and higher in magnitude for patients controls. This signifies that the brain activity in patient exhibits higher amount of activity than the controls.



(a)



(b)

Figure 2 Spatial connectivity signatures (above) and their corresponding temporal signatures (below) achieved from our machine learning approach for (a) controls and (b) patients. The connectivity signatures are coherence values among 68 brain regions. The temporal signatures are transient characteristics for that subgraph.

Analysis of each signature could be assessed by computing (3) and (4) for brain regions belonging to other standard subnetworks such as the visual, auditory, executive and salience subnetworks for computing their connectivity within their network and with the rest of the brain regions, which we keep for our future scope.

Furthermore, following (3) and (4), connectivity within the motor cortex and connectivity between the motor cortex and rest of the brain regions, as depicted in fig. 3, was comparatively in patients larger than that in controls on average by 16% and 0.8% respectively. Given that the subjects were not doing any tasks, we can be sure that higher connectivity does not correlate to constructive synchronous brain activity and hence implies that controls were able to inhibit the TMS subthreshold pulse whereas patients were not thereby signifying sensory gating deficits in patients.

IV. CONCLUSION AND FUTURE SCOPE

To conclude, it is essential to understand the underlying brain mechanisms in response to TMS for effective and safe treatment. We achieved this with unsupervised machine learning technique in high spatial and temporal resolution by using EEG based source localized connectivity data in response to TMS subthreshold pulse stimulus administered to left motor cortex in schizophrenia patients and healthy controls.

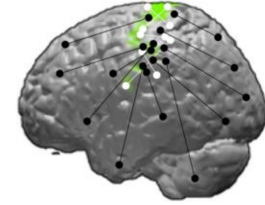


Figure 3 A depiction of connectivity within (white edges) motor cortex area and connectivity between the motor cortex and other parts of the brain (black edges) is shown. The motor cortex area is highlighted in green. Patients had higher connectivity activity than in controls thereby signifying sensory gating deficits.

More importantly, we successfully demonstrated that our results correlate to behavioral features i.e. the sensory gating deficits in patients. In future, we plan to extend our study to assessing subnetworks other than just the motor cortex for analyzing each signature in further detail.

APPENDIX

Here, we show a flowchart illustration of our methods in fig. 4.

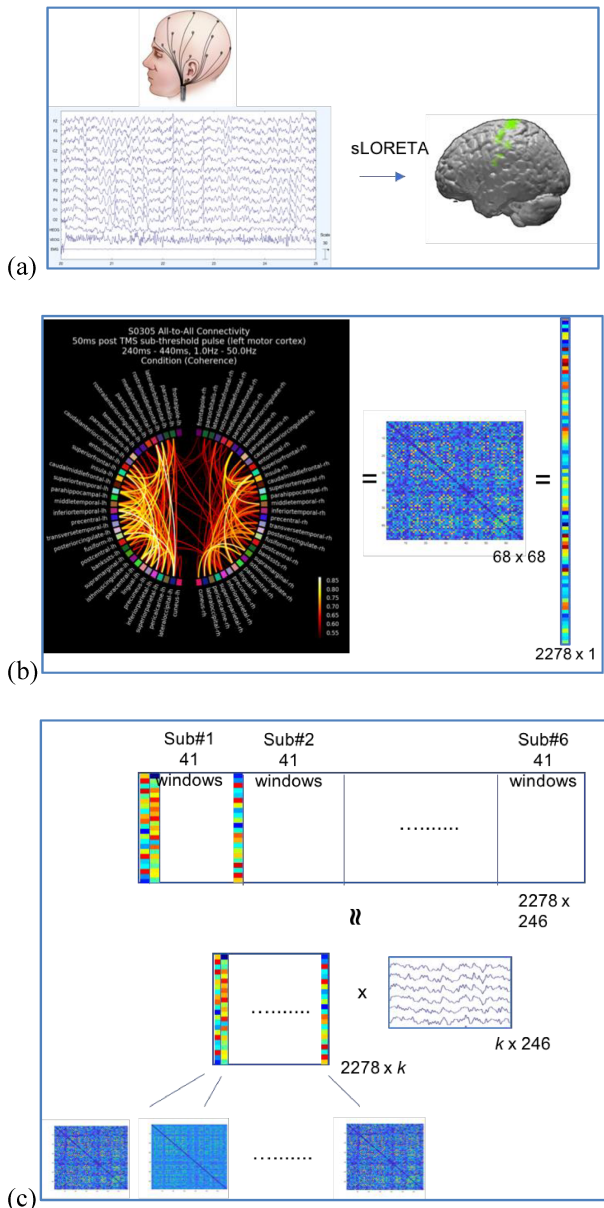


Figure 4 Illustration of our methods is shown here (a) After EEG recording and data preprocessing for artifact removal, we use sLORETA for 3D inverse projection to get source localization onto 68 regions inside the brain among which coherence is calculated with sliding window technique (b) coherence among 68 regions during one sample window for a sample subject is depicted in the form of a circular plot where the left sided semi-circle shows left hemisphere's regions and right sided semi-circle shows right hemisphere's regions. The high and low coherence values are shown by bright and dark colored connecting edges respectively. This connectivity data is equivalently a 68×68 symmetric matrix data that is flattened to a 2278×1 vector. (c) the flattened connectivity vector for all sliding window data of all subjects is stacked up as a 2278×246 matrix A , which is factorized by using NMF to get k spatial and temporal signatures namely, W and H respectively. Each vector in W corresponds to a subnetwork connectivity matrix and H contains the corresponding temporal signature.

REFERENCES

- [1] H. C. Cromwell, R. P. Mears, L. Wan, and N. N. Boutros, "Sensory gating: a translational effort from basic to clinical science," *Clin EEG Neurosci*, vol. 39, no. 2, pp. 69–72, Apr. 2008.
- [2] R. Freedman *et al.*, "Neurobiological Studies of Sensory Gating in Schizophrenia," *Schizophr Bull*, vol. 13, no. 4, pp. 669–678, Jan. 1987.
- [3] T. Perera, M. S. George, G. Grammer, P. G. Janicak, A. Pascual-Leone, and T. S. Wilecki, "The Clinical TMS Society Consensus Review and Treatment Recommendations for TMS Therapy for Major Depressive Disorder," *Brain Stimulation*, vol. 9, no. 3, pp. 336–346, May 2016.
- [4] A. Grinvald and R. Hildesheim, "VSDI: a new era in functional imaging of cortical dynamics," *Nature Reviews Neuroscience*, vol. 5, no. 11, pp. 874–885, Nov. 2004.
- [5] A. Delorme and S. Makeig, "EEGLAB: an open source toolbox for analysis of single-trial EEG dynamics including independent component analysis," *Journal of Neuroscience Methods*, vol. 134, no. 1, pp. 9–21, Mar. 2004.
- [6] J. Lopez-Calderon and S. J. Luck, "ERPLAB: an open-source toolbox for the analysis of event-related potentials," *Frontiers in human neuroscience*, vol. 8, p. 213, 2014.
- [7] R. D. Pascual-Marqui, "Standardized low-resolution brain electromagnetic tomography (sLORETA): technical details," *Methods Find Exp Clin Pharmacol*, vol. 24, no. Suppl D, pp. 5–12, 2002.
- [8] J. Talairach and P. Tournoux, "Co-planar stereotaxic atlas of the human brain: 3-dimensional proportional system: an approach to cerebral imaging," 1988.
- [9] G. Nolte, O. Bai, L. Wheaton, Z. Mari, S. Vorbach, and M. Hallett, "Identifying true brain interaction from EEG data using the imaginary part of coherency," *Clinical Neurophysiology*, vol. 115, no. 10, pp. 2292–2307, Oct. 2004.
- [10] A. Gramfort *et al.*, "MNE software for processing MEG and EEG data," *Neuroimage*, vol. 86, pp. 446–460, Feb. 2014.
- [11] A. Gramfort *et al.*, "MEG and EEG data analysis with MNE-Python," *Front. Neurosci.*, vol. 7, 2013.
- [12] H. Kim and H. Park, "Sparse non-negative matrix factorizations via alternating non-negativity-constrained least squares for microarray data analysis," *Bioinformatics (Oxford, England)*, vol. 23, no. 12, pp. 1495–1502, Jun. 2007.
- [13] N. Leonardi *et al.*, "Principal components of functional connectivity: A new approach to study dynamic brain connectivity during rest," *NeuroImage*, vol. 83, pp. 937–950, Dec. 2013.
- [14] L. R. Chai *et al.*, "Evolution of brain network dynamics in neurodevelopment," *Network Neuroscience*, vol. 1, no. 1, pp. 14–30, Feb. 2017.

ACKNOWLEDGMENT

We thank Corey Scheideman for his contribution.